Environmental Science and Pollution Research (2020) 27:23695–23706
https://doi.org/10.1007/s11356-020-08785-2

RESEARCH ARTICLE

MnOx-CuOx cordierite catalyst for selective catalytic oxidation of the NO at low temperature

Zhang Lei[1,2] · Shu Hao[3] · Lei Zhang[4] · Jia Yang[1] · Wang Yusu[5]

Received: 6 December 2019 / Accepted: 6 April 2020 / Published online: 15 April 2020

Abstract

Low-value solid waste cordierite honeycomb ceramics were used as carrier of SCO denitration catalyst, and the active component was supported by the impregnation method to improve the performance of the catalyst. Firstly, the effect of calcination conditions on the denitration performance of the Mn-loaded cordierite catalyst was studied for the cordierite-loaded active component MnO_X. Secondly, the preferred catalyst was reloaded with another active component to further improve its denitration performance; the bimetal ratios were affected by the denitration performance, which was, finally, characterized by XRD, XPS, and SEM. The result shows the following: (1) Mn-loaded cordierite prepared at 450 °C for 3 h has a good denitration effect; (2) the MnO_X-CuO_X/CR catalyst is superior to MnO_X-FeO_X/CR, MnO_X-CoO_X/CR, and MnO_X-CeO_X/CR; (3) the MnO_2 crystal form in the single metal-supported catalyst plays a major role, and $Cu_2Mn_3O_8$ in the bimetallic catalyst affects the performance and activity of the catalyst.

Keywords Selective catalytic oxidation · Cordierite · Catalyst · Denitration · Solid waste recycling · Resource utilization

Introduction

With the rapid development of the world economy, the living environment of mankind is increasingly facing a severe test, and the atmospheric environment on which we live has been seriously polluted (Wang et al. 2020). Nitrogen oxides (NO, NO_2, etc.) have many hazards and are one of the causes of air pollution problems (Wang et al. 2018; Liu et al. 2017; Zhang et al. 2019a, b). At this stage, China's large boilers mainly use coal as raw material (Rahman et al. 2019; Qiang et al. 2020; Zhang et al. 2020a, b, c). A large number of coal-fired power plants and nitrogen oxides emitted from steel-making boilers are one of the root causes of atmospheric pollution and photochemical smog, and their pollution hazards are widespread (Ashraf et al. 2019; Liu et al. 2019a, b; Chen et al. 2014). NO_X is not only the basis of nitric acid–type acid rain but also one of the main substances that form the greenhouse effect and destroy the ozone layer. It has strong toxicity and is harmful to human health, environment, ecology, and social and economic damage (Zhao et al. 2019a, b; Zhang et al. 2019a, b; Jogi et al. 2018). Therefore, the control of NO_X is imperative.

Responsible Editor: Vítor Pais Vilar

✉ Zhang Lei
leizh1981@sohu.com

Shu Hao
490258879@qq.com

Lei Zhang
leizh666@sohu.com

Jia Yang
519322049@qq.com

Wang Yusu
602222352@qq.com

[1] School of Geology and Environment, Xi'an University of Science and Technology, Xi'an 710054, China

[2] Key Laboratory of Coal Resources Exploration and Comprehensive Utilization, Ministry of Natural Resources, Xi'an 710021, China

[3] School of Water Resources and Hydroelectric Engineering, Xi'an University of Technology, Xi'an 710048, China

[4] China National Heavy Machinery Research Institute Co., Ltd., Xi'an 710032, China

[5] Shaanxi Weihe Ecological Zone Protection Center, Xi'an 710004, China

At present, selective catalytic reduction (SCR) technology, which uses ammonia as reducing agent to reduce NO to N_2, is the most commonly used method to remove NO_X from flue gas, but it has a high demand for catalyst (Han et al. 2019a, b; Liu et al. 2018). The successful SCR denitration catalyst is mainly a mixture of vanadium-titanium and tungsten trioxide or molybdenum trioxide (Wang et al. 2019a, b; Junhui et al. 2020; Song et al. 2020). Although vanadium-based catalysts have excellent activity and stability, they are also defective (Jiang et al. 2019; Song et al. 2019). The catalyst is only active in the temperature range of 380 to 450 °C. When the temperature is lower than 420 °C, the pores are blocked by the ammonium sulfate salt formed by the side reaction, and the activity is decreased (Jaegers et al. 2019; Tan et al. 2019; Zhao et al. 2019a, b). In addition, the cost of vanadium-titanium-type denitration catalyst is expensive, which is a significant expense for the enterprise.

Aiming at the shortcomings of the above SCR method, the selective catalytic oxidation (SCO) method for removing NO_X from the background of nitrogen oxides in boiler coal-fired flue gas is proposed**.** SCO is a flue gas purification technology that can simultaneously desulfurize and denitrify and can produce economical by-products. Since SCO does not require additional reducing gas, it has strong competitiveness (Liu et al. 2019a, b; Chen et al. 2017). SCO means that under the action of the catalyst, NO is partially oxidized to NO_2 by using oxygen in the flue gas, so that the oxidation degree (NO_2/NO_X) reaches 50 to 60% (at this time, the absorption efficiency is the highest) (Jablonska et al. 2018; Zhao et al. 2018; Tang et al. 2011). Then, the absorbent of wet desulfurization is used to realize wet desulfurization and denitration at the same time, and valuable by-products such as ammonium sulfate are generated by the self-oxidation and reduction of nitrogen oxides and sulfur oxides (Karthik et al. 2019). The method has low investment cost and low operating cost, and is compatible with the subsequent wet absorption process. The treatment efficiency can be as high as 99% or more, and it can generate economic benefits, and can simultaneously desulfurize and denitrify and reduce purification process and cost, and it will be the most valuable flue gas purification technology (Selvamani et al. 2017; Han et al. 2019a, b; Italiano et al. 2016). Since the SCO absorption method denitration has a catalytic oxidation process compared with the alkali denitration, this process greatly increases the denitration rate.

Like the SCR process, the catalyst is the core of the process. Choosing a catalyst with low temperature activity and low cost is essential for companies to reduce their costs and increase their benefits (Zhang et al. 2020a, b, c). At present, most of denitration catalysts are supported catalysts, and most of the carriers are materials with large pore structure, such as molecular sieve and active carbon (Vita et al. 2018; Wen et al. 2019). Compared with other kinds of catalysts, mordenite has good acid and corrosion resistance, which is suitable for some specific denitration processes (Moskovskaya et al. 2019). Activated carbon catalyst and molecular sieve catalyst have high activity for catalytic oxidation of NO at low temperature, and even have large conversion rate at room temperature, but molecular sieve and activated carbon are complicated in preparation and high in cost (Xu et al. 2020). Therefore, it is of great research significance and use value to choose a carrier with low price to obtain stable performance. In recent years, more and more researchers hope to use the solid waste produced in industry to prepare high-performance functional materials. Cordierite raw materials prepared from industrial solid waste or mined tailings are easily available due to their low cost. Also, preparing it as a catalyst can reduce the cost of the catalyst and improve its utilization (Yi et al. 2018; Zhu et al. 2019; Abdelhamid 2019).

Cordierite is often used as a refractory because of its high mechanical properties and high thermal stability. More and more solid waste is used to prepare cordierite materials, and we used the prepared commercial cordierite honeycomb ceramics in this paper. Based on our research on cordierite (Zhang et al. 2020a, b, c), in this experiment, the low-value cordierite was used as the carrier and different metal components as the active components to prepare an efficient catalyst for low-temperature SCO denitration processes, which not only realized the utilization of solid waste resources but also achieved the reduction of industrial flue gas, achieving a win-win situation.

Experimental

Experimental device

The activity evaluation of the catalyst is shown in Fig. 1.

Methods

Materials

The cordierite used in this experiment is a honeycomb ceramic material. Moreover, it has great mechanical strength and needs to be cut into 0.5-cm pieces during the laboratory test. It took 3 groups of 5 g cordierite, and they were put into a 100-mL beaker. Distilled water was added until the cordierite was completely immersed and sealed. After 24 h, when the cordierite was saturated, it was taken out and weighed and the average value calculated; the saturated water absorption of cordierite was 1.373 g.

The preparation of the catalyst

1. The cordierite was cut into the cubic with a side length of about 5 mm.

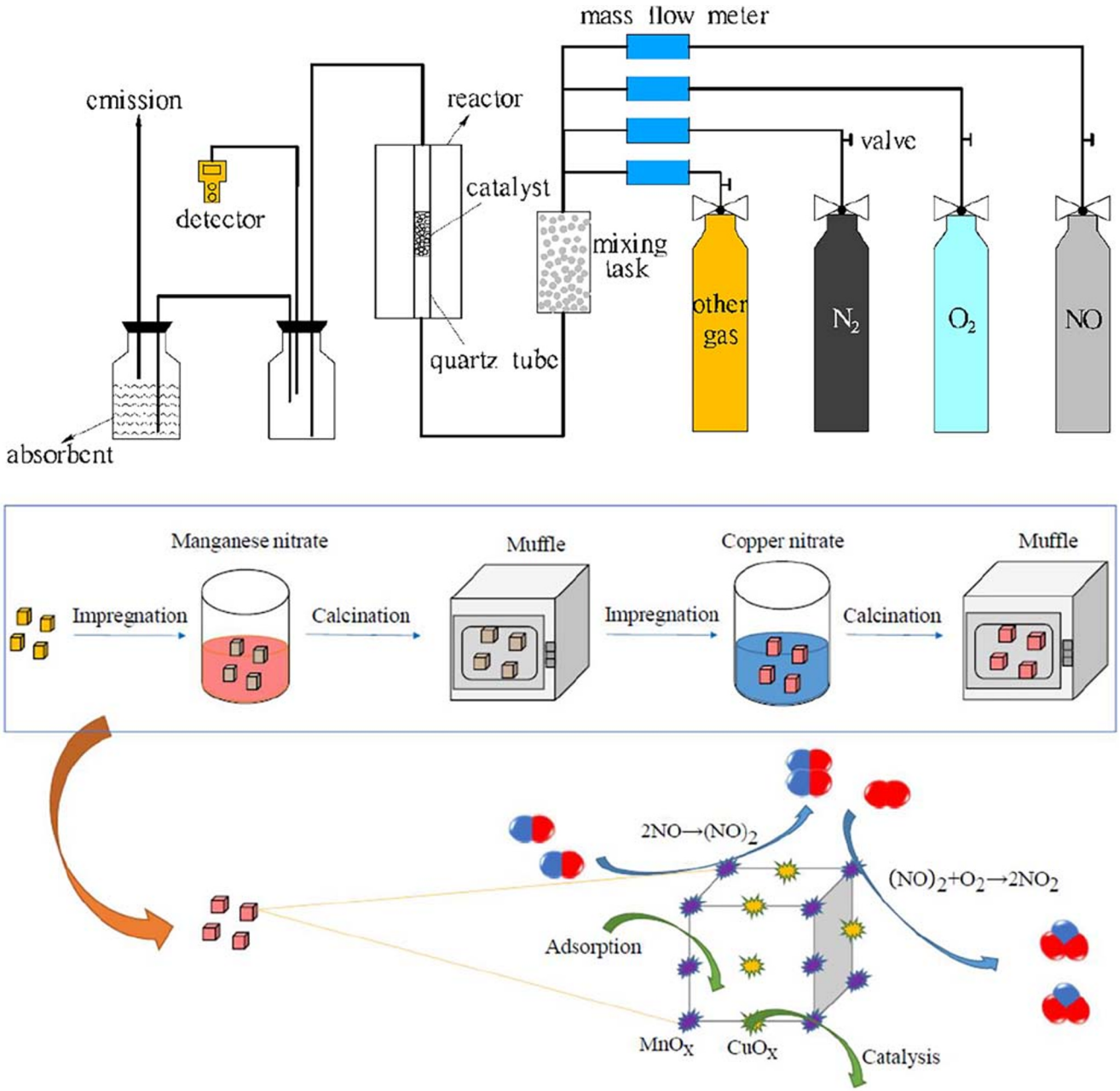

Fig. 1 Catalyst activity evaluation experimental process

2. One percent of Mn was loaded on the cordierite using an equal-volume impregnation method, and the loaded samples were calcined in the muffle furnace at 350 °C, 450 °C, and 550 °C to investigate the optimum calcination temperature of the cordierite catalyst. In order to investigate the optimum calcination time, the loaded sample was calcined in the muffle furnace for 2 h, 3 h, and 4 h under the condition of the optimum calcination temperature.
3. Under the optimal calcination conditions, the fixed Mn/X (X = Cu, Co, Fe, Ce), the loading ratio was 2:1. The second metal on the MnOx catalyst was immersed by distributed impregnation, and the optimal bimetallic supported catalyst was obtained.
4. The optimal bimetal obtained in (3) was adjusted to the Mn/X load ratio: 1:2, 1:3, 1:5, 5:1, 3:1, 2:1, 2:3, 3: 2; the optimal loading ratio of the bimetallic supported catalyst was investigated.

Flue gas analysis and evaluation system

In this experiment, the temperature of the reactor was set to 150 °C, and the total amount of gas was 1000 mL/min, in

which nitrogen monoxide was 600 ppm, oxygen was 6%, and the rest was nitrogen.

Different catalysts were placed in the temperature control tower, and the change in NO was detected and recorded by a flue gas analyzer (Testo 340).

The calculation method of the denitration rate is as follows:

$$\text{Removal efficiency} = \frac{C_{NO_{inlet}} - C_{NO_{outlet}}}{C_{NO_{inlet}}} \times 100\% \quad (1)$$

Experimental characterization

XRD The sample was tested by an XD-3 X-ray diffraction analyzer to obtain an XRD pattern. The composition of grains and materials formed on the surface of the catalyst was observed, and the denitration mechanism was studied from the viewpoint of catalyst crystallites and dispersion.

SEM Secondary electron signal imaging was used to capture the characteristics of the surface of the sample; that is, the sample was scanned with a particularly narrow electron beam, causing the two to interact and produce an effect. The secondary electrons magnify the topography of the sample surface, which was created chronologically as the sample scanned. In this paper, the SEM model was JSM-6460LV, the working voltage was 20 kV, and the magnification was 5000 times.

XPS The sample was X-rayed to excite inner electrons (or valence electrons) in the atoms (or molecules). Photons could excite photoelectrons (energy measurable) and obtain the composition of the analyte through photoelectron spectroscopy. The X-ray photoelectron spectrometer model used in this paper was ESCALAB 250 (manufactured by Thermo Fisher Scientific, USA). The instrument had a sensitivity of 180 KCPS, an energy resolution of 0.45 eV (Ag), and an image resolution of 3 μm. The results of the analysis were all corrected with C1s.

Results and discussion

Effect of calcination conditions on denitration performance of MnOx/CR catalysts

Effect of calcination time on denitration performance of MnOx/CR catalyst

Three sets of 5 g cordierite catalyst loaded with 1% Mn were weighed and placed in the muffle furnace at 450 °C for calcination, and the calcination time was set to 2 h, 3 h, and 4 h, respectively. The calcined catalyst was added to the SCO denitration apparatus for denitration experiments, then the optimum calcination time was screened; the results are shown in Fig. 2a.

It can be seen from Fig. 2a that the denitration rate increases first and then decreases with the extension of the calcination time. When the calcination time is short, the metal substance supported on the catalyst surface does not react with oxygen sufficiently, and manganese nitrate cannot be oxidized into oxide form of manganese completely, so the denitration effect is not obvious. Moreover, since the calcination time is short, the catalyst does not form a uniform pore structure, and the denitration effect is also low. As the calcination time is prolonged, the contact time of the catalyst with oxygen increases, and nitrate can be fully oxidized, so the uniformly pore structure is formed, and the denitration effect is best. However, when the calcination time is too long, the smaller pore structure in the catalyst is continuously destroyed, resulting in the disappearance of many smaller pores. Moreover, the active sites are reduced, shortening the residence time of the flue gas in the catalyst, weakening the catalytic effect of the catalyst, so the denitration effect decreases. In summary, when the calcination time is 3 h, the denitration effect is best.

Effect of calcination temperature on denitration performance of MnOx/CR catalyst

Three sets of 5 g cordierite catalyst loaded with 1% Mn were weighed and placed in the muffle furnace for 3 h, and the calcination temperature was set at 350 °C, 450 °C, and 550 °C, respectively. The calcined catalyst was added to the SCO denitration apparatus for experiments, so the optimum calcination time was screened; the results are shown in Fig. 2b.

It can be seen from Fig. 2b, that the denitration rate increases first and then decreases with the calcination temperature increasing. When the calcination time is short, the metal substance supported on the catalyst surface does not react with oxygen sufficiently. Moreover, manganese nitrate cannot be oxidized into the oxide form of manganese completely, and the active site on the catalyst surface is formed incompletely, so the denitration effect is not obvious. When the calcination temperature increases, the active component of the catalyst is capable of reacting with oxygen sufficiently. Therefore, nitrate can be fully oxidized, the more active site is formed, and the denitration effect is best. When the calcination temperature is too high, the manganese oxide in the catalyst is destroyed, and the better pore structure and active site is destroyed. The active component in the metal oxide is deactivated, resulting in poor denitration effect. In summary, when the calcination temperature is 450 °C, the denitration effect is best.

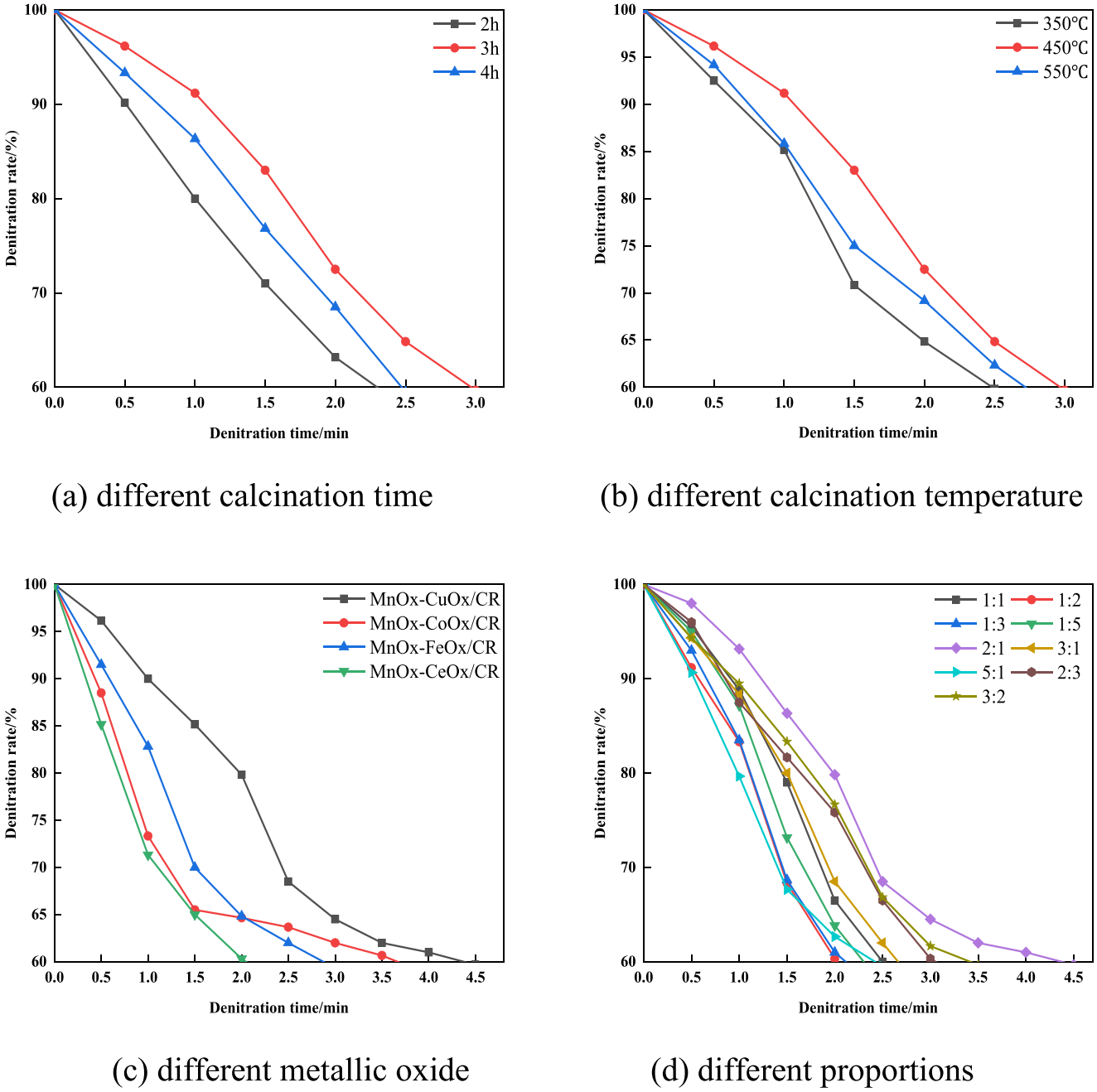

Fig. 2 Effect of different conditions on denitration of catalysts

Effect of denitration performance of the bimetallic MnO_X-CuO_X/CR catalyst

Effect of different metal supported catalysts on denitration performance

Four sets of 5 g cordierite catalyst loaded with 1% Mn were weighed, and the nitrates were selected as cerium nitrate, ferric nitrate, copper nitrate, and cobalt nitrate. Moreover, the cordierite catalyst is impregnated in an equal volume as the ratio 2:1. The catalyst was placed in the muffle furnace, and the calcination temperature was set at 450 °C, the calcination time 3 h. The calcined catalyst was added to the SCO denitration device for experiments, and the optimum bimetallic ratio was screened. The results are shown in Fig. 2c.

It can be seen from Fig. 2c that the effect of the bimetallic catalyst on denitration is obviously improved. It can be seen that the denitration effect of the MnO_X-CuO_X/CR catalyst is optimal. This is because the Mn-based catalyst has a good activity, but its conversion rate of converting NO to NO_2 is still very low at 150 °C, which cannot meet

the requirements of industrial applications. Therefore, we choose the method of doping the second metal to improve the activity of the catalyst and achieve the purpose of converting NO into NO_2. It can be seen from Fig. 2c that, when the metal Cu oxide is added to synergistic denitration, the Cu-based catalyst synergizes with the Mn-based catalyst to increase the oxygen adsorption capacity of the catalyst, and promotes the conversion of NO to NO_2 in the flue gas, thereby improving the denitration effect.

The denitration mechanism of Cu oxide synergistic Mn-based catalyst is

$$2MnO_2 \rightarrow Mn_2O_3 + O \quad (2)$$

$$Mn_2O_3 + 2CuO \rightarrow 2MnO_2 + Cu_2O \quad (3)$$

$$Cu_2O + O \rightarrow 2CuO \quad (4)$$

The reaction between MnO_2 and Mn_2O_3 can effectively enhance the oxidation effect of the catalyst. The O transfer between CuO and Mn_2O_3 enhances the reaction. Therefore, the bimetallic supported Mn/Cu catalyst has a better denitration effect.

Effect of bimetallic load ratio on denitration performance of MnO_X-CuO_X/CR catalyst

Nine groups of 5 g cordierite were weighed, and the ratio of MnO_X/CuO_X loaded on the catalyst was 1:1, 1:2, 1:3, 1:5, 2:1, 3:1, 5:1, 2:3, and 3:2. The calcination temperature was set to 450 °C, the calcination time to 3 h, and the calcined catalyst was added to the SCO denitration device for experiments to screen out the optimal loading ratio of bimetal. The results are shown in Fig. 2d.

It can be seen from Fig. 2d that the catalyst with different loading ratios has a significant denitration effect. It can be seen that when the ratio of MnO_X/CuO_X is 2:1, the denitration effect of the catalyst is optimal. This is because MnO_2 plays a major denitration role, and CuO is mainly used for storing and releasing the oxygen. When the ratio of MnO_X/CuO_X is less than 2:1, a large amount of CuO occupies the active site of the reaction, which reduces the active site of MnO_2, so that NO cannot fully react with the active site of MnO_2, and the denitration effect is poor. When the ratio of MnO_X/CuO_X is more than 2:1, the amount of MnO_2 is too large, occupying the active site of reaction. After the reaction shown in Eq. (2), the reaction shown in Eqs. (3) and (4) cannot be effectively promoted, and the adjustment of CuO cannot achieve the oxygen demand of the active sites of MnO_2, thereby the denitration effect of the catalyst decreased.

Characterization

Characterization of XRD

(1) XRD analysis of MnOx/CR catalysts with different calcination conditions Figure 3a shows the XRD patterns of the cordierite catalysts prepared at different calcination times. It can be seen that the morphology and amount of metal oxide formed on the surface of the supported catalyst prepared at different calcination times are different. As the calcination time increases, the crystal of manganese oxide increases, and the main crystal is MnO_2. When the calcination time is 2 h, the manganese nitrate is not completely oxidized into manganese oxide due to the short calcination time, and the manganese oxide crystal is less, so the denitration effect is poor. When the calcination time is 3 h, manganese nitrate is completely oxidized into manganese oxide, which has more MnO_2 crystal and a better activity. Therefore, the denitration effect is good when the calcination time is 3 h. When the calcination time is 4 h, although there are many manganese oxides, the MnO_2 crystal with better activity is oxidized to MnO crystal. Therefore, the denitration effect of 4 h is not as good as that of 3 h. Combined with the difference between the calcination time of the catalyst and the denitration efficiency, we can conclude the following: under different calcination time conditions, the denitrification effect and activity of the catalysts prepared are different. The denitration rate of the catalysts prepared at different times is 3 h > 4 h > 2 h, so the optimum time for calcination is 3 h.

Figure 3b shows the XRD patterns of the cordierite catalysts prepared at different calcination temperatures. It can be seen that the cordierite catalysts prepared at different temperatures have different metal oxide valence states on the surface. The higher the calcination temperature, the lower the valence state of the metal manganese. With the calcination temperature increasing, the oxidation of manganese oxide is $MnO_2 \rightarrow Mn_2O_3 \rightarrow MnO$, and the activity order of metal manganese oxide is $MnO_2 > Mn_2O_3 > MnO$. When the temperature is 350 °C, the manganese nitrate is not completely calcined to form an oxide structure of manganese. When the calcination temperature is 550 °C, manganese nitrate is completely oxidized, but a lot of MnO crystal is formed, so its activity is rather lowered. When the calcination temperature is 450 °C, there is the most MnO_2 crystal in the surface, and the catalyst has the best activity (Yangxian et al. 2020; Veerapandian et al. 2019). In addition, manganese oxide peaks have fewer sharp peaks; it is indicated that the large crystal of manganese oxide does not appear, and the dispersion of manganese oxide on the cordierite catalyst is better. Moreover, when the calcination temperature is 450 °C, there are many kinds of manganese oxides, among which there are more peaks of MnO_2; many manganese oxides having different valence states can be formed during the reaction, and the activity is the best.

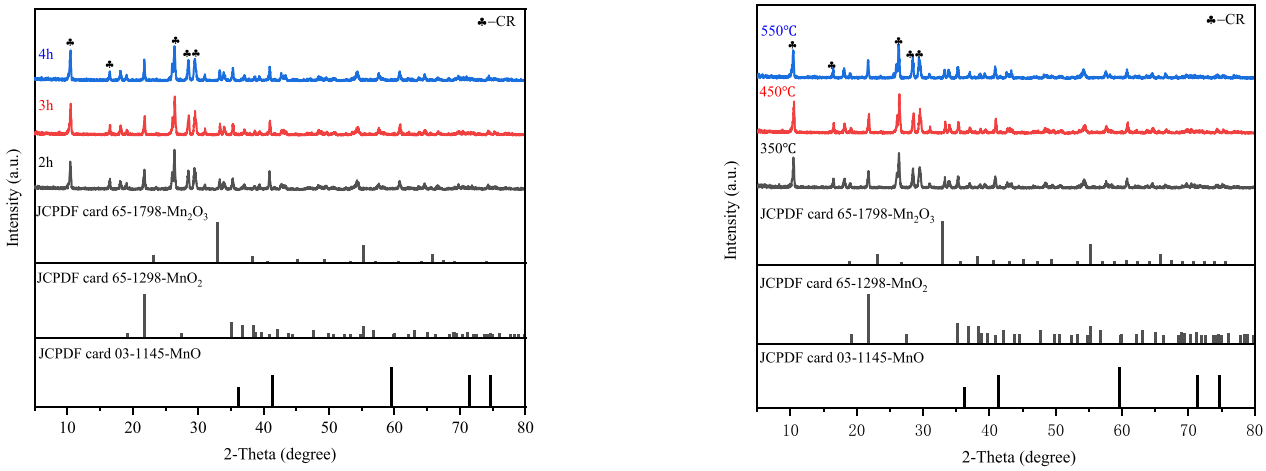

(a) different calcination time (b) different calcination temperatures

Fig. 3 XRD patterns of MnOx/CR catalysts with different calcination conditions

From the relationship between the catalyst preparation temperature and the denitration performance, the catalysts prepared under different calcination temperatures have a denitration rate of 450 °C > 550 °C > 350 °C. It is indicated that there are many mixed valence oxides on the catalyst surface, and when the crystal structure of MnO_2 is large, the denitration effect is better, so the optimum calcination temperature is 450 °C.

(2) XRD analysis of different bimetallic supported catalysts

From the results shown in Fig. 2d, the MnO_X-CuO_X/CR bimetallic supported catalyst has the best denitration effect.

It can be seen from Fig. 2d that CuO is highly dispersed on the catalyst surface after the loading of Cu, and it can be seen from Fig. 4a that the crystal structure of $Cu_2Mn_3O_8$ is formed on the catalyst surface due to the bimetallic loading. It is speculated that CuO and Mn_2O_3 enhance the reaction synergistically, and $Cu_2Mn_3O_8$ crystals play a major catalytic role.

When the metal oxide is non-stoichiometric, or when impurity ions or atoms are introduced, an N-type, P-type semiconductor can be produced. Impurities are distributed in the crystal structure of the metal oxide by ions, atoms, or groups, mainly at the crystal surface or the lattice junction. There may be the impurity level in the semiconductor band gap due to these impurities. An N-type semiconductor is an impurity semiconductor in which the concentration of free electrons is significantly larger than the hole concentration. The impurity provides negatively charged electron carriers, known as N-type impurities (Maurya et al. 2019). In the N-type semiconductor, free electrons are majority carrier, and holes are a minority carrier; it is mainly conductive by free electrons. Since the amount of positive and negative charges in the N-type semiconductor is equal, the N-type semiconductor exhibits electrical neutrality. Free electrons are mainly formed by impurity atoms, and the holes are formed by thermal excitation. The more impurities are incorporated, the more the concentration of free electrons, and the better the conductivity. The hole of the P-type semiconductor is a majority carrier, and the free electron is a minority carrier, so that it is mainly conducted by holes. Since the amount of positive and negative charges in the P-type semiconductor is equal, the P-type semiconductor is electrically neutral (Wang et al. 2019a, b). The holes are mainly formed by impurity atoms, and the free electrons are formed by thermal excitation. The more impurities are incorporated, the higher the concentration of holes, and the higher the conductivity, so the oxidation performance is higher.

The reason is that MnO_2 is an N-type metal oxide, and its Mn is in the +4 valence state, which is higher than the +2 valence state of Cu. Therefore, when CuO crystal is added to the MnO_2 crystal, the conductivity is improved due to the increase in concentration of free electrons, so the catalytic effect is enhanced. In addition, the catalyst has structural defects due to the formation of the $Cu_2Mn_3O_8$ crystal structure, which causes the concentration of free electrons to increase in turn, resulting in an enhanced catalytic effect. It can be seen from Fig. 4b–d that the main crystal oxides formed are Fe_2O_3, Co_3O_4, and Ce_2O_3 when metal Fe, Co, and Ce are introduced. Since Fe_2O_3, Co_3O_4, and Ce_2O_3 are P-type semiconductors, the introduction of Fe_2O_3, Co_3O_4, and Ce_2O_3 into the MnO_2 catalyst increases the hole concentration and decreases the concentration of free electrons, resulting in the conductivity decrease and inactivation of the catalyst. Combined with Fig. 2c, it can be concluded that the MnO_X-CuO_X/CR catalyst has the best denitration effect.

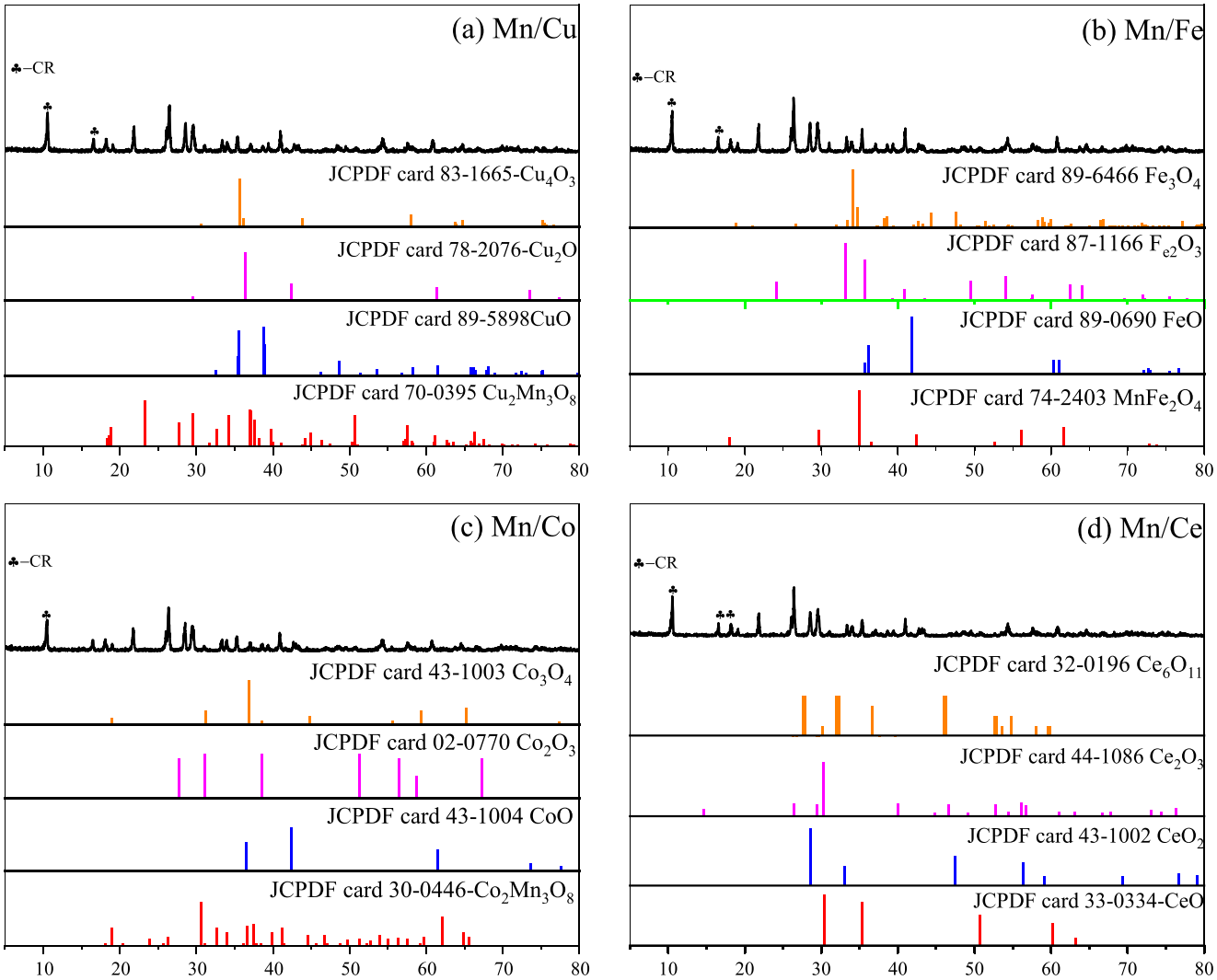

Fig. 4 XRD patterns of different metal loadings

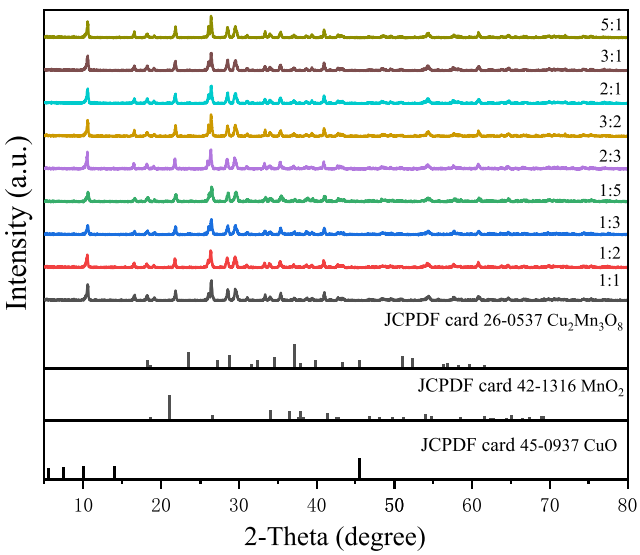

Fig. 5 XRD pattern of MnO_X-CuO_X/CR catalysts with different loading ratios

It can be seen from Fig. 5 that when the MnO_X/CuO_X loading ratio is 2:1, the distribution of MnO_2, CuO, and $Cu_2Mn_3O_8$ is the most uniform, and the crystals of the metal oxides are mainly MnO_2 and CuO. According to the previous analysis, MnO_2 is a P-type metal oxide. Therefore, CuO crystal is added to the crystal structure of MnO_2, so that the concentration of free electrons increases, and the conductivity is increased, so that the catalytic effect is enhanced. In addition, the catalyst structure has defects due to the formation of $Cu_2Mn_3O_8$, which will cause the concentration of free electrons increasing. When the MnO_X/CuO_X loading ratio is more than 2:1, the crystal structure of MnO_2 increases, which occupies more active sites on the catalyst surface, and weakens the O transfer between CuO and Mn_2O_3, resulting in the decrease in the denitration rate. When the MnO_X/CuO_X loading ratio is less than 2:1, the CuO crystal formed on the catalyst surface increases, occupying the active site in the catalyst. Because the MnO_2 crystal is the main role in the denitration process, the activity of the catalyst is lowered when CuO

occupies the reactive site, resulting in a decrease in the denitration rate. Therefore, when the MnO_X/CuO_X loading ratio is 2:1, the denitration effect is the best.

Characterization of SEM

Figure 6 is an SEM analysis with different conditions.

From the comparison between Fig. 6a–d, it can be seen that the obvious crystal structure is formed on the catalyst surface after the catalyst is supported by the metal. Combined with Fig. 3a, the crystal structure is assumed to be MnO_2. When the calcination time is 2 h, the manganese nitrate supported on the catalyst was completely calcined to manganese oxide, and thus the crystal structure is not remarkable. When the calcination time is 3 h, the crystal structure is relatively complete and the dispersion is uniform. When the calcination time is 4 h, since the calcination time is too long, the catalyst crystal structure is burned, resulting in the catalyst activity decreasing. Therefore, it can be inferred that the catalyst effect is optimal when the calcination time is 3 h.

It can be seen from Fig. 6e–g that the significant crystal structure is formed on the catalyst surface after loading MnO_X. It can be concluded that the crystal structure is MnO_2. When the calcination temperature is 350 °C, manganese nitrate in the catalyst is completely calcined to manganese oxide. When the calcination temperature is 450 °C, the crystal structure is relatively complete and uniform dispersion. When the calcination temperature is 550 °C, since the calcination temperature is too high, the crystal structure of the catalyst is burned, resulting in a decrease in catalyst activity. Combined with Fig. 3b, it can be inferred that the catalyst effect is optimal when the calcination temperature is 450 °C.

Figure 6h is an SEM image of the MnO_X-CuO_X/CR catalyst. MnOx and CuOx are supported on the catalyst in a ratio of 2: 1. Moreover, it can be inferred that the crystallinity of MnO_X is higher and the crystal structure of CuO_X is less in Fig. 6h. Combined with Fig. 5, the two crystal structures have more MnO_2 crystals and less CuO crystals. The interaction of the two crystal structures increases the concentration of free electrons and the conductivity. Therefore, the catalytic effect is enhanced due to the increase in catalytic activity, and the denitration effect is increased.

XPS analysis of MnO_X-CuO_X/CR catalyst

It can be seen from Fig. 7 that the binding energy of $Mn2p_{3/2}$ is 639.110 eV and 642.820 eV, respectively. The binding energies of $Mn2p_{1/2}$ are 651.116 eV and 654.724 eV, respectively. The Mn at the position of 639.140 eV and 651.116 eV is analyzed in the form of Mn^{3+}. The surface of the Mn_2O_3 crystal can be analyzed by XRD. The Mn at the position of

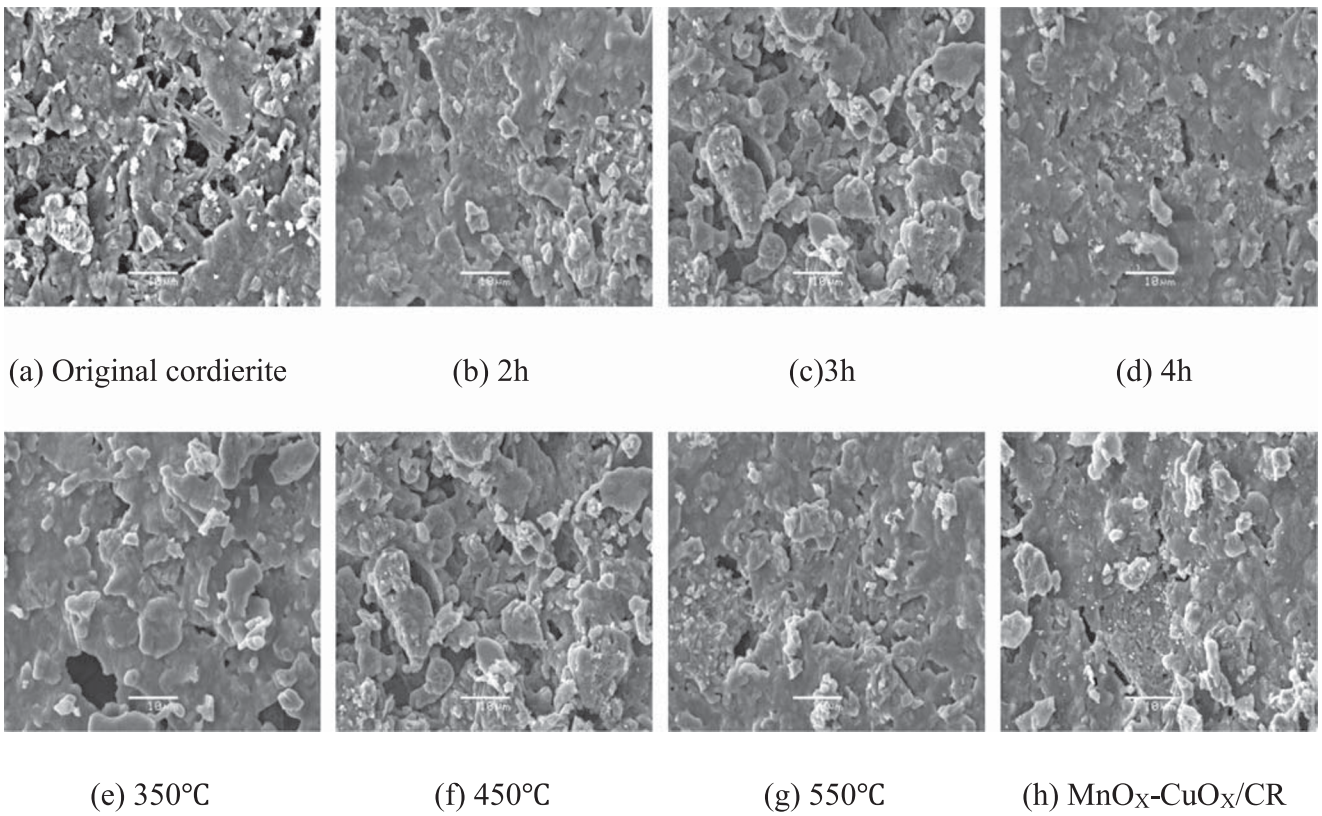

Fig. 6 SEM of different conditions

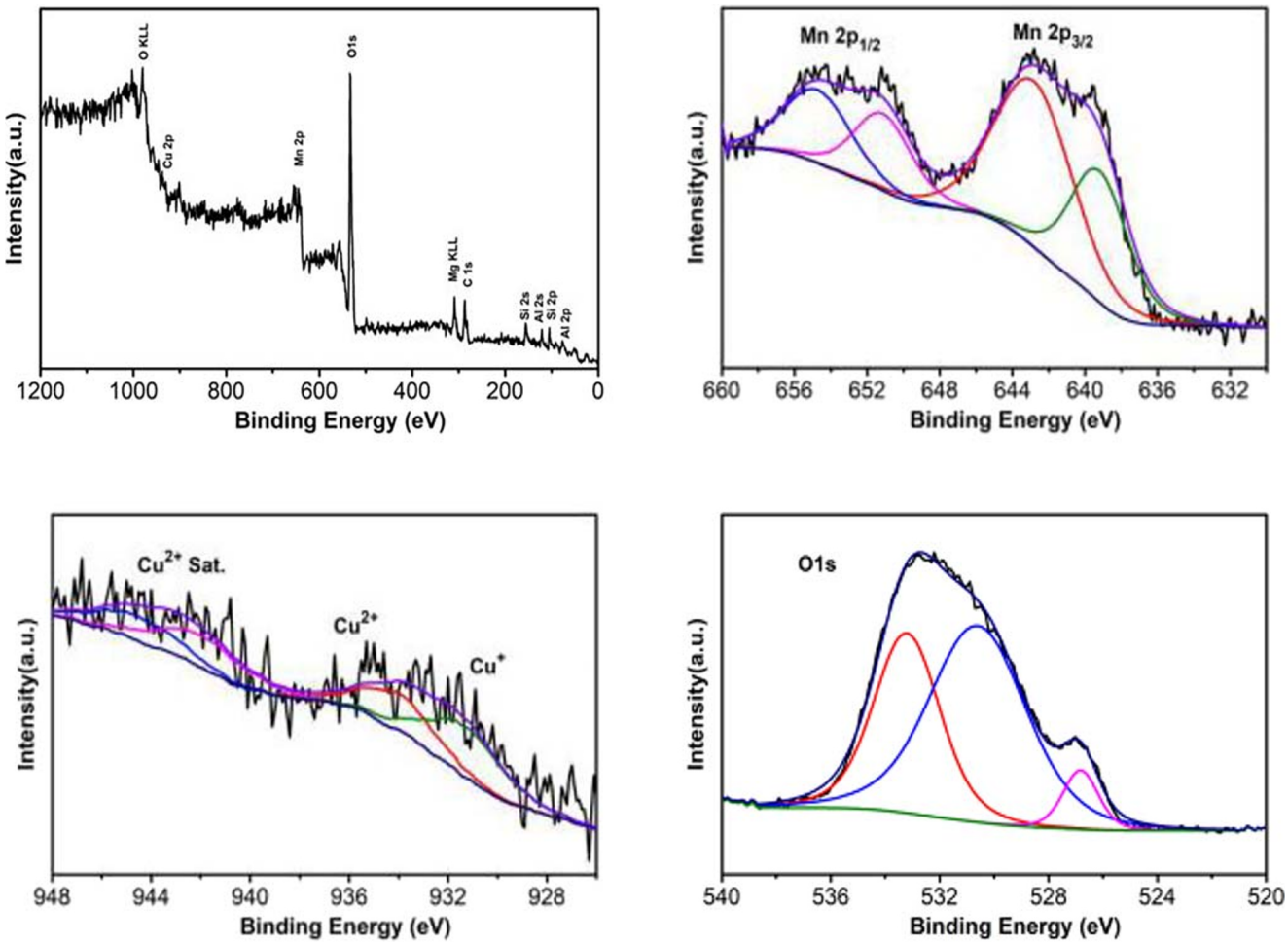

Fig. 7 The XPS of MnO_X-CuO_X/CR catalyst

639.140 eV and 651.116 eV is Mn^{4+}; combined with the XRD analysis, it is mainly the action of the surface MnO_2 crystal.

It can be seen that the binding energy of $Cu2P_{3/2}$ is 936.302 eV and 939.045 eV, respectively. The Cu in the position of 936.303 eV is analyzed in the form of Cu^+. Combined with XRD, it is mainly CuO_2 crystal by analyzing. At the position of 939.045 eV, Cu exists in the form of Cu^{2+}, and combined with XRD, it is CuO crystal by analyzing.

It can be seen from the O-peak diagram that the binding energies of O1s are 526.823 eV, 530.609 eV, and 533.208 eV, respectively. At 526.823 eV and 530.609 eV, it is O^{2-} (lattice oxygen); at 533.208 eV, oxygen O_2^{2-} (or O^-) strongly adsorbs. As can be seen from Table 1, the lattice oxygen/adsorbed oxygen in the catalyst is 1.77. This is because MnO_2 is a P-type metal oxide; its Mn is in the +4 valence state, higher than the +2 valence state of Cu, and CuO is a P-type semiconductor. Therefore, CuO crystal is added to the crystal structure of MnO_2, so that the concentration of free electrons rises, the conductivity is increased, and thus the catalytic effect is enhanced. In addition, the catalyst produces structural defects due to the formation of the $Cu_2Mn_3O_8$ crystal structure; this kind of defect will increase the concentration of free electrons, which is conducive to the generation of adsorbed oxygen. The adsorbed oxygen has a strong mobility and plays an important role in the performance and activity of the catalyst.

Table 1 XPS analysis table of MnO_X-CuO_X/CR catalyst O

Catalyst	Lattice oxygen/adsorbed oxygen
MnO_X-CuO_X/CR	1.77

Conclusion

The solid waste cordierite undergoes certain treatment or processing, and its altered form plays an important role in the SCO denitration process. Comprehensive utilization of solid waste makes it a secondary resource available. In this paper, the low value solid waste cordierite was used as a catalyst carrier, and Mn-based oxide was used as the active component, the optimum preparation conditions were selected by

changing the calcination time and the calcination temperature. Based on the optimal preparation conditions, different metals were used to explore the optimal bimetal load combination and load ratio. The denitration of the MnO_X-CuO_X/CR catalyst was analyzed. The result shows the following:

1. The calcination conditions will affect the denitration effect of the catalyst; the optimum calcination time is 3 h, and the optimum calcination temperature is 450 °C.
2. The effects of different metals and Mn on bimetallic loading are also different, and the effect of Cu is relatively better than that of Fe, Ce, and Co.
3. The MnO_X-CuO_X/CR catalyst has a significant denitration effect when the load ratio is 2:1.
4. When the loading ratio of MnO_X/CuO_X is 2:1, the distribution of MnO_2, CuO, and $Cu_2Mn_3O_8$ is the most uniform, and the crystal shape of the metal oxide is mainly MnO_2 and CuO.

Author contribution Conceptualization, Lei Zhang (F) and Zhang Lei(M); methodology, Shu Hao; software, Jia Yang; validation, Wang Yusu and Shu Hao; investigation, Zhang Lei(M); data curation, Shu Hao; writing-original draft preparation, Wang Yusu; writing-review & editing, Shu Hao.

Funding information This research was funded by the National Natural Science Foundation of China [grant number 51704230 and 41907255]; Key Laboratory of Coal Resources Exploration and Comprehensive Utilization, Ministry of Natural Resources in P.R. China [grant number KF2019-7]; Shannxi Key Research and Development Project [grant number 2019ZDLSF05-05-01]; 2019 Shaanxi Provincial Natural Science Basic Research Program Enterprise Joint Fund Project [grant number 2019JL-01]; Natural Science Basic Research Plan in Shaanxi Province of China [grant number 2018JM5048]; and Xi'an Science and Technology Plan Project [grant number 2019217714GXRC013CG014-GXYD13.4].

Compliance with ethical standards

Conflict of interest The authors declare that they have no conflict of interest.

References

Abdelhamid HN (2019) Surfactant assisted synthesis of hierarchical porous metal-organic frameworks nanosheets. Nanotechnology 30:43. https://doi.org/10.1088/1361-6528/ab30f6

Ashraf A, Butt A, Khalid I, Alam RU, Ahmad SR (2019) Smog analysis and its effect on reported ocular surface diseases: a case study of 2016 smog event of Lahore. Atmos Environ 198:257–264. https://doi.org/10.1016/j.atmosenv.2018.10.029

Chen M, Jin L, Liu Y, Guo XR, Chu JW (2014) Decomposition of NO in automobile exhaust by plasma–photocatalysis synergy. Environ Sci Pollut Res 21(2):1242–1247. https://doi.org/10.1007/s11356-013-2021-2

Chen MY, Zhao MM, Tang FS, Ruan L, Yang B (2017) Effect of Ce doping into V_2O_5-WO_3/TiO_2 catalysts on the selective catalytic reduction of NOx by NH. J Rare ERarth 35:1206–1215. https://doi.org/10.1016/j.jre.2017.06.004

Han J, Kim T, Jung H, Pyo S, Cho G, Oh Y, Kim H (2019a) Improvement of NO_X reduction rate of urea SCR system applied for an non-road diesel engine. Int J Auto Tech-Kor 20:1153–1160. https://doi.org/10.1007/s12239-019-0108-6

Han W, Yi HH, Tang XL, Zhao SZ, Gao FY, Zhang XD, Ma CB, Song LL (2019b) Mn-Fe-Ce coating onto cordierite monoliths as structured catalysts for NO catalytic oxidation. ChemistrySelect 4:4664–4671. https://doi.org/10.1002/slct.201900834

Italiano C, Balzarotti R, Vita A, Latorrata S, Fabiano C, Pino L, Cristiani C (2016) Preparation of structured catalysts with Ni and Ni Rh/CeO_2 catalytic layers for syngas production by biogas reforming processes. Catal Today 273:3–11. https://doi.org/10.1016/j.cattod.2016.01.037

Jablonska M, Wolkenar B, Beale AM, Pischinger S, Palkovits R (2018) Comparison of Cu-Mg-Al-O-x and Cu/Al_2O_3 in selective catalytic oxidation of ammonia (NH_3-SCO). Catal Commun 110:5–9. https://doi.org/10.1016/j.catcom.2018.03.003

Jaegers NR, Lai JK, He Y, Walter E, Dixon DA, Vasiliu M, Chen Y, Wang CM, Hu MY, Mueller KT, Wachs IE, Wang Y, Hu JZ (2019) Mechanism by which tungsten oxide promotes the activity of supported V_2O_5/TiO_2 catalysts for NO_X abatement: structural effects revealed by V-51 MAS NMR spectroscopy. Angew Chem Int Ed 58:12609–12616. https://doi.org/10.1002/anie.201904503

Jiang LJ, Liu QC, Ran GJ, Kong M, Ren S, Yang J, Li JL (2019) V_2O_5-modified Mn-Ce/AC catalyst with high SO_2 tolerance for low-temperature NH_3-SCR of NO. Chem Eng J 320:810–821. https://doi.org/10.1016/j.cej.2019.03.225

Jogi I, Erme K, Levoll E, Raud J, Stamate E (2018) Plasma and catalyst for the oxidation of NOx. Plasma Sources Sci T 27(3). https://doi.org/10.1088/1361-6595/aaae3c

Junhui Z, Sun G, Liu J, Evrendilek F, Buyukada M (2020) Co-combustion of textile dyeing sludge with cattle manure: assessment of thermal behavior, gaseous products, and ash characteristics. J Clean Prod 253:119950

Karthik K, Devi KRS, Pinheiro D, Sugunan S (2019) Photocatalytic activity of bismuth silicate heterostructures synthesized via surfactant mediated sol-gel method. Mater Sci Semicond Process 102. https://doi.org/10.1016/j.mssp.2019.104589

Liu YX, Wang Y, Liu ZY, Wang Q (2017) Oxidation removal of nitric oxide from flue gas using UV photolysis of aqueous hypochlorite. Environ Sci Technol 51:11950–11959. https://doi.org/10.1021/acs.est.7b03628

Liu YX, Liu ZY, Wang Y, Yin YS, Pan JF, Zhang J, Wang Q (2018) Simultaneous absorption of SO_2 and NO from flue gas using ultrasound/Fe^{2+}/heat coactivated persulfate system. J Hazard Mater 342:326–334. https://doi.org/10.1016/j.jhazmat.2017.08.042

Liu C, Li F, Wu J, Hou X, Huang W, Zhang Y, Yang XG (2019a) A comparative study of MOx (M = Mn, Co and Cu) modifications over $CePO_4$ catalysts for selective catalytic reduction of NO with NH_3. J Hazard Mater 363:439–446. https://doi.org/10.1016/j.jhazmat.2018.09.054

Liu JY, Sun MM, Lin QJ, Liu S, Xu HD, Chen YQ (2019b) Promotional effects of ethylenediamine on the low-temperature catalytic activity of selective catalytic oxidation of ammonia over Pt/SiAlOx: states and particle sizes of Pt. Appl Surf Sci 481:1344–1351. https://doi.org/10.1016/j.apsusc.2019.03.199

Maurya KC, Biswas B, Garbrecht M, Saha B (2019) Wave-vector-dependent Raman scattering from coupled plasmon-longitudinal optical phonon modes and Fano resonance in n-type scandium nitride. Phys Status Solid-R 13:9. https://doi.org/10.1002/pssr.201900196

Moskovskaya IF, Romanovskii BV, Russ (2019) Molecular-Sieve catalysis: pioneering works of the chemists of Moscow State University. Russ J Phys Chem A 93:1859–1864. https://doi.org/10.1134/S0036024419100194

Qiang S, Hongyu Z, Jinwei J, Li Y, Wen L, Qiuxiang G, Xinqian S (2020) Effects of demineralization on the surface morphology, microcrystalline and thermal transformation characteristics of coal. J Anal Appl Pyrolysis 145:104716. https://doi.org/10.1016/j.jaap.2019.104716

Rahman M, Rooney R, Hara K, Nakatani S (2019) Measurement of automobile NO from bag and continuous stream by quantum cascade laser spectroscopy. Int J Eng Res 20:261–273. https://doi.org/10.1177/1468087417750937

Selvamani A, Shanthi K, Santhanaraj D, Babu CM, Srinivasan VV, Thirukumaran P, Ramkumar V, Shakilaparveen A, Balasubramanian R (2017) Effective removal of automobile exhausts over flower-like Ce1-xCuxO_2 nanocatalysts exposed active {100} plane. J Rare Earths 36(6):603–612. https://doi.org/10.1016/j.jre.2017.12.006

Song Q, Zhao HY, Jia JW, Zhang F, Wang ZP, Lv W, Yang L, Zhang W, Zhang Y, Shu XQ (2019) Characterization of the products obtained by pyrolysis of oil sludge with steel slag in a continuous pyrolysis-magnetic separation reactor. Fuel 255:115711. https://doi.org/10.1016/j.fuel.2019.115711

Song Y, Hu J, Liu JY, Evrendilek F, Buyukada M (2020) Catalytic effects of CaO, Al_2O_3, Fe_2O_3, and red mud on Pteris vittata combustion: emission, kinetic and ash conversion patterns. J Clean Prod 252:119646. https://doi.org/10.1016/j.jclepro.2019.119646

Tan PQ, Wang SY, Hu ZY, Lou DM (2019) Durability of V_2O_5-WO_3/TiO_2 selective catalytic reduction catalysts for heavy-duty diesel engines using B20 blend fuel. Energy 179:383–391. https://doi.org/10.1016/j.energy.2019.04.149

Tang N, Liu Y, Wang HQ, Wu ZB (2011) Mechanism study of NO catalytic oxidation over MnOX/TiO_2 catalysts. J Phys Chem C 115:8214–8220. https://doi.org/10.1021/jp200920z

Veerapandian SKP, Ye ZP, Giraudon JM, De Geyter N, Morent R, Lamonier JF (2019) A plasma assisted Cu-Mn mixed oxide catalysts for trichloroethylene abatement in moist air. J Hazard Mater 379:120781. https://doi.org/10.1016/j.jhazmat.2019.120781

Vita A, Italiano C, Ashraf MA, Pino L, Specchia S (2018) Syngas production by steam and oxy-steam reforming of biogas on monolith-supported CeO_2-based catalysts. Int J Hydrog Energ 43:11731–11744. https://doi.org/10.1016/j.ijhydene.2017.11.140

Wang H, Zhong HY, Bo GZ (2018) Existing forms and changes of nitrogen inside of horizontal subsurface constructed wetlands. Environ Sci Pollut Res 25(1):771–781. https://doi.org/10.1007/s11356-017-0477-1

Wang Y, Liu YX, Liu Y (2019a) Elimination of nitric oxide using new Fenton process based on synergistic catalysis: optimization and mechanism. Chem Eng J 372:92–98. https://doi.org/10.1016/j.cej.2019.04.122

Wang JY, Nie ZG, An ZW, Bai HC, Wang FY, Zhang XL, Li YH, Wang CP (2019b) Improvement of SO_2 resistance of low-temperature Mn-based denitration catalysts by Fe doping. ACS Omega 4:3755–3760. https://doi.org/10.1021/acsomega.9b00002

Wang H, Wang J, Lu H, Bo GZ, Zhang XY, Cao YQ, Lu L, Zhang JS, Zhang W (2020) Analysis of coating electrode characteristics in the process of removing pollutants from wastewater. Fresenius Environ Bull 29(2):715–721

Wen CL, Wang XM, Xu JD, Fan Y (2019) Hierarchical SAPO-11 molecular sieve-based catalysts for enhancing the double-branched hydroisomerization of alkanes. Fuel 255. https://doi.org/10.1016/j.fuel.2019.115821

Xu JQ, Zhang C, Guo F, Chen Z, Xie JQ, Liu QC, Xi WC, Yang J (2020) Preparation of the coupling co-precipitation and impregnation catalyst Ag/Al_2O_3 with high catalytic performance in selective catalytic reduction of NO with C_3H_6. J Nanosci Nanotechnol 20:1170–1176. https://doi.org/10.1166/jnn.2020.16971

Yangxian L, Ye S, Yan W (2020) Novel simultaneous removal technology of NO and SO_2 using a semi-dry microwave activation persulfate system. Environ Sci Technol 54:2031–2042. https://doi.org/10.1021/acs.est.9b07221

Yi HH, Huang YH, Tang XL, Zhao SZ, Gao FY, Xie XZ, Wang JG, Yang ZY (2018) Synthesis of Mn-CeOx/cordierite catalysts using various coating materials and pore-forming agents for non-methane hydrocarbon oxidation in cooking oil fumes. Ceram Int 44:15472–15477. https://doi.org/10.1016/j.ceramint.2018.05.203

Zhang L, Chen JH, Zhang L, He HB, Wang YS, Li YH (2019a) Preparation of soybean oil factory sludge catalyst and its application in selective catalytic oxidation denitration process. J Clean Prod 225:220–226. https://doi.org/10.1016/j.jclepro.2019.03.254

Zhang L, Jia Y, Zhang L, He HB, Yang C, Luo M, Miao LT (2019b) Preparation of soybean oil factory sludge catalyst by plasma and the kinetics of selective catalytic oxidation denitrification reaction. J Clean Prod 217:317–323. https://doi.org/10.1016/j.jclepro.2019.01.182

Zhang L, Gao H, Chang X, Zhang L, Wen X, Wang YS (2020a) An application of green surfactant synergistically metal supported cordierite catalyst in denitration of selective catalytic oxidation. J Clean Prod 249:119307. https://doi.org/10.1016/j.jclepro.2019.119307

Zhang L, Jia Y, Shu H, Zhang L, Wen X, Luo M, Wang YS, Xu D (2020b) Application of surfactant-modified cordierite-based catalysts in denitration process. Fuel 268:117242

Zhang L, Shu H, Zhang L, Jia Y (2020c) Gas modified pyrolysis coke for in-situ catalytic cracking of coal tar. ACS Omega. https://doi.org/10.1021/acsomega.0c00055

Zhao HY, Song Q, Liu SC, Li YH, Wang XH, Shu XQ (2018) Study on catalytic co-pyrolysis of physical mixture/staged pyrolysis characteristics of lignite and straw over an catalytic beds of char and its mechanism. Energ Convers Manag 161:13–26. https://doi.org/10.1016/j.enconman.2018.01.083

Zhao HY, Li YH, Song Q, Liu SC, Ma QX, Shu XQ (2019a) Catalytic reforming of volatiles from co-pyrolysis of lignite blended with corn straw over three different structures of iron ores. J Anal Appl Pyrolysis 144:104714. https://doi.org/10.1016/j.jaap.2019.104714

Zhao HY, Li YH, Song Q, Liu SC, Yan J, Ma QX, Ma L, Shu XQ (2019b) Investigation on the thermal behavior characteristics and products composition of four pulverized coals: its potential applications in coal cleaning. Int J Hydrog Energ 42:23620–23638. https://doi.org/10.1016/j.ijhydene.2019.07.087

Zhu J, Zhang GM, Qi QP, Xian G, Zhang N, Li JW (2019) A high-efficiency CuO/CeO_2 catalyst for diclofenac degradation in Fenton-like system. Front Chem 7. https://doi.org/10.3389/fchem.2019.00796